

# Polymer gel electrolytes containing sulfur-based ionic liquids in lithium battery applications at room temperature

Mingtao Li · Bolun Yang · Zhan Zhang ·  
Lu Wang · Ying Zhang

Received: 17 October 2012 / Accepted: 7 February 2013 / Published online: 21 February 2013  
© Springer Science+Business Media Dordrecht 2013

**Abstract** Polymer gel electrolytes comprising a sulfur-based ionic liquid (IL), a lithium salt, and butyrolactone (GBL) as an additive hosted in PVdF-HFP matrix were prepared and characterized. The result shows that adding small amount of GBL to the polymer electrolytes can improve the cathodic stability of the electrolytes, which ensures the lithium plating/stripping in the redox process. Furthermore, cyclic voltammograms studies indicate that the polymer electrolytes have well reversible redox process. When the IL component reaches 75 wt%, the polymer electrolyte has higher ionic conductivity than the other samples and it is  $6.32 \times 10^{-4} \text{ S cm}^{-1}$ . The assembled batteries with the polymer electrolyte have better discharge capacity, and after 100 cycles, the discharge capacity of the battery still retains 148 mAh  $\text{g}^{-1}$ .

**Keywords** Lithium polymer batteries · Polymer gel electrolytes · Sulfur-based ionic liquids

## 1 Introduction

Ionic liquids (ILs), namely low temperature molten salts, have drawn much interest in view of their unique properties as new types of safety electrolytes in electrochemistry [1, 2]. The unique properties include non-volatility, non-flammability, high ionic conductivity, and wide temperature range of operation. The replacement of conventional volatile organic solutions with the ILs electrolytes can reduce risks

of thermal runaway and, eventually, fire accidents, thus finally improving the safety of the batteries [3]. Recently, the research of switching ILs to IL-based polymer electrolytes has been extensively examined.

Hence, variety of imidazolium-based and pyrrolidinium-based ILs were synthesized and incorporated into polymer matrix [4–8]. These imidazolium-based ILs have low cathodic stability and an unfavorable compatibility toward the lithium metal anode due to the presence of acidic protons and double bonds in the cation. Small quantities of film-forming additives have to be added in the electrolyte to avoid its cathodic decomposition and to improve the interfacial compatibility toward the lithium anode [9, 10]. In comparison with the imidazolium-based ILs, pyrrolidinium-based ILs show a much wider cathodic decomposition potential and better compatibility toward the lithium anode. For example, electrochemical properties of the incorporation of several *N*-alkyl-*N*-methypyrrolidinium bis(trifluoromethane-sulfonyl)imide ( $\text{PYR}_{1\text{A}}\text{TFSI}$ ) ILs into PEO-based electrolytes system had been reported [4]. The addition of  $\text{PYR}_{1\text{A}}\text{TFSI}$  enhanced the ionic conductivity of PEO-based electrolytes over  $10^{-4} \text{ S cm}^{-1}$ . Battery tests had shown that discharge capacity was 125 and 100 mAh  $\text{g}^{-1}$  at 30 and 25 °C, respectively. In addition, PVdF–HFP composite membranes incorporated lithium bis(trifluoromethane-sulfonyl)imide ( $\text{LiTFSI}$ ), ether-functionalized pyrrolidinium-imide IL ( $\text{PYRA}_{1201}\text{TFSI}$ ), and different silica had been prepared, and their electrochemical properties had been investigated also [11].

However, for IL-based polymer electrolytes, much work has been devoted to imidazolium-based and pyrrolidinium-based ILs, and the other ILs such as sulfur-based ILs have been seldom discussed [12]. In this study, a sulfur-based IL was synthesized due to its low viscosity, high room temperature conductivity, and high solubility of lithium salts [4–7]. Polymer electrolytes incorporating the sulfur-based

M. Li (✉) · B. Yang · Z. Zhang · L. Wang · Y. Zhang  
State Key Laboratory of Multiphase Flow in Power Engineering,  
School of Chemical Engineering and Technology, Xi'an  
Jiaotong University, Xian 710049, Shaanxi, China  
e-mail: lmt01558@mail.xjtu.edu.cn

IL, LiTFSI, and butyrolactone (GBL) as film-forming additives hosted in PVdF–HFP matrix were prepared and characterized. The performance of the polymer electrolytes in Li/LiFePO<sub>4</sub> batteries cycling at room temperature was reported.

## 2 Experimental

### 2.1 Materials

Ethyl sulfide, butyrolactone (GBL), and iodomethane were purchased from Alfa Aesar. Lithium bis(trifluoromethylsulfonyl) imide (LiTFSI) kindly provided by Morita Chemical Industries Co., Ltd., Poly(vinylidene fluoride-*co*-hexafluoropropylene) (PVdF–HFP, average  $M_w \sim 400,000$ ) were purchased from Sigma-Aldrich. All the other chemicals used in the study were of A.R. grade.

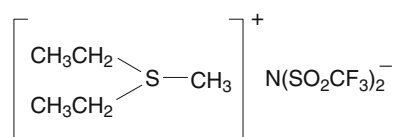
### 2.2 Synthesis of the IL, S221TFSI

Trialkylsulfonium iodides were prepared according to the reference method [13]. The produced iodides and LiTFSI were dissolved in deionized water and mixed for 24 h at ambient temperature. The obtained crude IL, S221TFSI (see Scheme 1), was dissolved with dichloromethane, and washed with deionized water until no residual iodide anions in the deionized water were found, which were detected with the solution of AgNO<sub>3</sub>. The dichloromethane was removed by rotating evaporation. Then, S221TFSI was dried under high vacuum for more than 24 h at 100 °C. The water content of the dried IL was detected by a moisture titrator (Metrohm 73KF coulometer) based on Karl–Fischer method, and the value was less than 100 ppm. The structures of synthesized ILs were confirmed by <sup>1</sup>H NMR and <sup>13</sup>C NMR (Mercury Yplus 400) and [D<sub>6</sub>] acetone for the IL. The characterization data are as follows:

S221TFSI: <sup>1</sup>H NMR:  $\delta$  (ppm) 3.52–3.36 (m, 4H), 2.97 (s, 3H), 1.52–1.47 (t, 6H); <sup>13</sup>C NMR:  $\delta$ (ppm) 124.92–115.40, 35.33, 20.67, 8.07;

### 2.3 Preparation of the polymer electrolyte

The polymer electrolyte was prepared by the solution casting method. Firstly, LiTFSI salt was dissolved into a certain proportion of S221TFSI/GBL solution to form a



**Scheme 1** The structure of S221TFSI

0.8 mol kg<sup>−1</sup> liquid electrolyte. The resulting IL solution was then mixed with 10 wt% PVdF–HFP acetone solution resulting in a viscous mixture. The weight ratio of the lithium salt/S221TFSI/GBL (SE) to PVdF–HFP was set at 7:3, 3:1, and 4:1, respectively (see Table 1). Finally, the mixture solution was cast over a Teflon tray, and the acetone was subsequently evaporated under vacuum at 60 °C for 12 h resulting in a freestanding polymer electrolyte membrane.

### 2.4 Characterization of the polymer electrolyte

Electrochemical stability was determined by the linear sweep voltammetry (LSV) of a Li/the electrolyte membrane/Stainless steel (SS) cell at a scan rate of 10 mV s<sup>−1</sup> over the range of open-circuit voltage to 6.0 V. The decomposition voltage onset was set as the current density which was up to 0.1 mA cm<sup>−2</sup> [14].

The ionic conductivity of the samples was measured by sandwiching the samples between two SS blocking electrodes using AC impedance techniques. The measurements were performed using a CHI660D Electrochemical Workstation between 100 kHz and 10 Hz at various temperatures ranging from 25 to 60 °C. A thermostatic equipment (Jinghua Co., Ltd., Shanghai, China) was utilized to control the temperature within  $\pm 0.1$  °C of the target value. The samples were thermally equilibrated at each temperature for at least 1 h prior to the measurements. The bulk resistance ( $R_b$ ) was obtained by reading the intercept of the impedance spectrum, and the ion conductivity was calculated from the expression  $\sigma = L/(R_b A)$  where  $L$  is the thickness of the electrolyte film and  $A$  represents the electrode area.

Cyclic voltammetry (CV) of the polymer gel electrolyte membrane sandwiched between lithium electrodes was measured at 25 °C at a scan rate of 10 mV s<sup>−1</sup> between −0.5 and +2.6 V, respectively.

Lithium ion transference number,  $T_{Li+}$ , was evaluated using the method originally proposed by Vincent and Bruce [15, 16]. The electrolyte film was sandwiched between two lithium-unblocking electrodes to form a symmetric Li/polymer gel electrolyte/Li cell. The coin cell (CR2016) was assembled and sealed in the argon-filled glove box. Measurements were performed using a CHI660D Electrochemical Workstation. The method consists of initial measurement of the lithium interfacial resistance ( $R_0$ ) by the impedance spectroscopy in the 1 MHz  $\sim$  0.1 Hz frequency range, application of a small voltage (10 mV) until a steady current was obtained ( $I_{ss}$ ), and final measurement of the interfacial resistance ( $R_f$ ) by impedance spectroscopy in the 1 MHz  $\sim$  0.1 Hz frequency range.  $T_{Li+}$  was calculated using the following equation:

**Table 1** Composition of the polymer gel electrolytes

Sample set	Weight composition (wt%)				PVdF/SE ratio wt/wt	GBL/SE ratio wt/wt	LiTFSI/SE ratio mol/wt
	PVdF	SE					
		S221TFSI	GBL	LiTFSI			
Sam A	30	47	7	16	30/70	1/10	0.08
Sam B	25	50.5	7.5	17	25/75	1/10	0.08
Sam C	20	54	8	18	20/80	1/10	0.08
Sam Blank	25	58	0	17	25/75	0	0.08

The PVdF-HFP/SE (PVdF/SE), GBL/SE, and LiTFSI/SE ratios (in weight and in mol) are reported for comparison

$$T_{\text{Li}^+} = \frac{I_{\text{ss}}}{I_0} \left( \frac{\Delta V - I_0 R_0}{\Delta I_{\text{ss}} R_{\text{f}}} \right),$$

where  $\Delta V$  means the applied polarization voltage and  $I_0$  means the initial current and was calculated from the voltage and the overall cell resistance by

$$I_0 = \frac{\Delta V}{R_{\text{b}} + R_0},$$

where  $R_{\text{b}}$  was the bulk resistance of the PIL.

## 2.5 Evaluation of the performance of cells

Li/LiFePO<sub>4</sub> coin cell was used to evaluate the performance of the polymer electrolytes in lithium battery applications. Lithium foil (battery grade) was used as a negative electrode. The thickness and surface area of the lithium foil were 1.2 mm and 1.54 cm<sup>2</sup>, respectively. The positive electrode was fabricated by spreading the mixture of LiFePO<sub>4</sub>, acetylene black, and PVdF (initially dissolved in *N*-methyl-2-pyrrolidone) with a weight ratio of 8:1:1 onto Al current collector (battery use). Loading of active material was about ca. 2.0–2.5 mg cm<sup>−2</sup>, and this thinner electrode was directly used without pressing. Cell construction was carried out in the glove box, and all the components of cell were dried under vacuum before being placed into the glove box. Cell performance was examined by the galvanostatic charge–discharge (C-D) cycling test using a CT2001A cell test instrument (LAND Electronic Co., Ltd.) at 25 and 50 °C. The cells were sealed and then stayed at determining temperature for 12 h before the performance test. Current rate was determined using the nominal capacity of 169 mAh g<sup>−1</sup> for Li/LiFePO<sub>4</sub> cell. Charge included two processes: (1) constant current at a rate, cut-off voltage of 4.0 V and (2) constant voltage at 4.0 V, setting time of 2 h, and discharge had one process: constant current at different rates, cut-off voltage of 2.5 V.

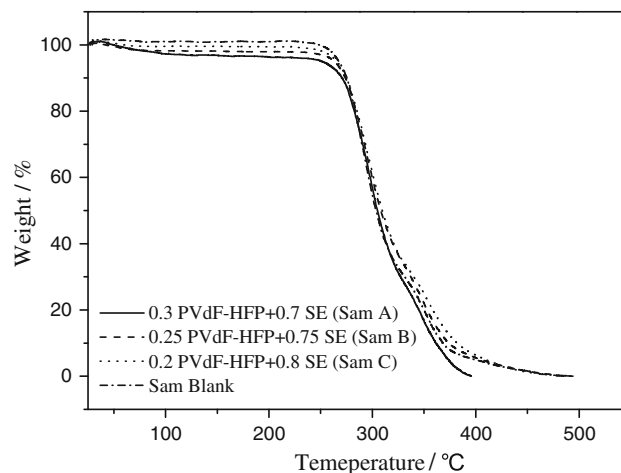


**Fig. 1** TGA profiles of  $x$ PVdF-HFP/(1− $x$ ) SE ( $x = 0.3, 0.25$ , and  $0.2$ ) polymer gel electrolytes

## 3 Results and discussion

### 3.1 Thermal stability

The thermal stability of the polymer gel electrolytes with different S221TFSI amounts was characterized by TGA, as shown in Fig. 1. The polymer gel electrolytes containing GBL additives exhibited a small weight loss of <5 % before significant weight loss, which was presumably due to the evaporation of GBL that the samples were loaded. Furthermore, it was known that the content of GBL additives in the polymer gel electrolytes was retained about 5 wt% after vacuum drying process. On the other hand, the gel electrolyte samples showed similar thermal decomposition behaviors, and they all decomposed in two steps. Decomposition of the polymer gel electrolytes started at around 290 and 350 °C, corresponding to the decomposition of S221TFSI [13] and PVdF-HFP [17] in the electrolytes.

### 3.2 Ionic conductivity

Figure 2 shows the temperature dependence of the ionic conductivity of polymer electrolyte samples. For the

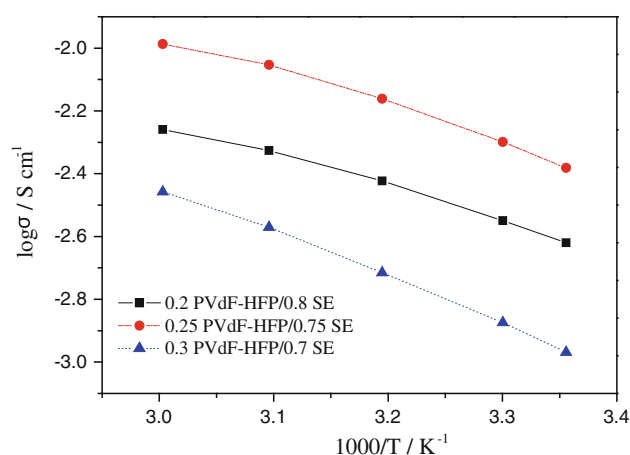


**Fig. 2** Temperature dependence of the ionic conductivity of xPVdF-HFP/(1-x) SE ( $x = 0.3, 0.25$ , and  $0.2$ ) polymer gel electrolytes

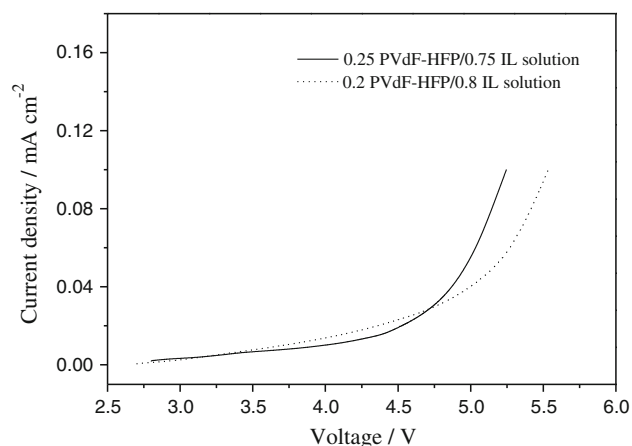


**Fig. 3** Electrochemical stability of xPVdF-HFP/(1-x) SE ( $x = 0.25$  and  $0.2$ ) polymer electrolytes. (Li/polymer electrolyte/SS cell,  $10 \text{ mV s}^{-1}$ ,  $2.7\text{--}5.5 \text{ V}$ )

samples, the temperature dependence of conductivity is gradually changed from an Arrhenius-like relationship to a more VTF (Vogel–Tamman–Fulcher)-like relationship when the contents of S221TFSI were increased. The variation of ionic conductivity following Arrhenius-like behavior (the conductivity curve is much straighter) indicates that ion mobility is coupled with the segmental motion of the polymer chain at lower S221TFSI contents [18]. At higher S221TFSI contents, the conductivity curve becomes more bended, i.e., more VTF-like. The fact that the conductivity perfectly follows a VTF behavior implied that the motion of charged species, anions and cations, is controlled by the viscous properties of the IL [19].

In addition, it was also obvious from Fig. 2 that the ionic conductivity enhanced markedly with increasing the IL content, which was attributed to the increase of charged species from S221TFSI. However, it had a certain

threshold of 75 wt% SE, and below the threshold, the ionic conductivity rapidly begins to decrease, which was also reported by previous paper [11]. The origin of the decay in conductivity at higher S221TFSI concentration could be due to both changes in the morphology, i.e., size and connectivity of the pores in the membrane, and/or interactions between the IL and the polymer matrix [19].

The polymer electrolytes 0.25 PVdF-HFP/0.75 SE and 0.2 PVdF-HFP/0.8 SE exhibited high ionic conductivity above  $6.32 \times 10^{-4}$  and  $4.78 \times 10^{-4} \text{ S cm}^{-1}$  at  $25^\circ\text{C}$ , respectively, which proved them suitable for the application in lithium polymer batteries at room temperature. Since the two kinds of samples had higher ionic conductivity, the next electrochemical characterization was performed with them.

### 3.3 Electrochemical stability and chemical stabilities against lithium metal

Electrochemical stabilities of the PIL-based electrolyte samples at  $25^\circ\text{C}$  were characterized by LSV, as shown in Fig. 3. The IL content did not obviously affect the electrochemical stability of the PIL-based electrolytes. They decomposed at about  $4.2 \text{ V}$  versus  $\text{Li/Li}^+$  (here the potential limit was set at a current density up to  $0.1 \text{ mA cm}^{-2}$ ), which was suitable for the application in  $\text{Li/LiFePO}_4$  battery as a polymer gel electrolyte at room temperature.

The Li/polymer gel electrolyte/Li symmetric cells were used to investigate the chemical stabilities of the IL electrolyte against the lithium metal and the interfacial characteristics between the Li metal electrode and the polymer gel electrolytes by the electrochemical impedance spectra (EIS). Figure 4a, b illustrated the time dependence of impedance spectra for Li/IL electrolyte/Li symmetric cells under the open circuit conditions. The intercept with the real axis of the response at high frequency was assigned to electrolyte bulk resistance ( $R_{\text{bulk}}$ ), and the diameter of the semicircle was related to the interfacial resistance ( $R_i$ ) of the polymer gel electrolyte/lithium metal, as explained in the literature [10]. For the Sam Blank electrolyte, its  $R_{\text{bulk}}$  was almost unchanged during the testing period of 24 h. The  $R_i$  increased gradually from 0 h to 16 h, and the  $R_i$  reached about  $17,500 \Omega$  after 16 h, which could be seen in Fig. 5. The cause of the high interfacial resistance could be that the cathodic limiting potential of S221TFSI was about  $1.6 \text{ V}$  versus  $\text{Li/Li}^+$  [13], so that the polymer gel electrolyte would continuously react with lithium metal. However, for the Sam B electrolyte, its  $R_{\text{bulk}}$  and  $R_i$  were both increased gradually from 0 to 3 h and from 0 to 16 h, respectively. The  $R_{\text{bulk}}$  and  $R_i$  retained about  $500 \Omega$  and  $1,800 \Omega$  after 3 and 16 h, respectively, which was also illustrated in Fig. 5. The lower interfacial resistance might indicate that the additive GBL in the Sam B electrolyte could react with lithium metal and a passivation film could

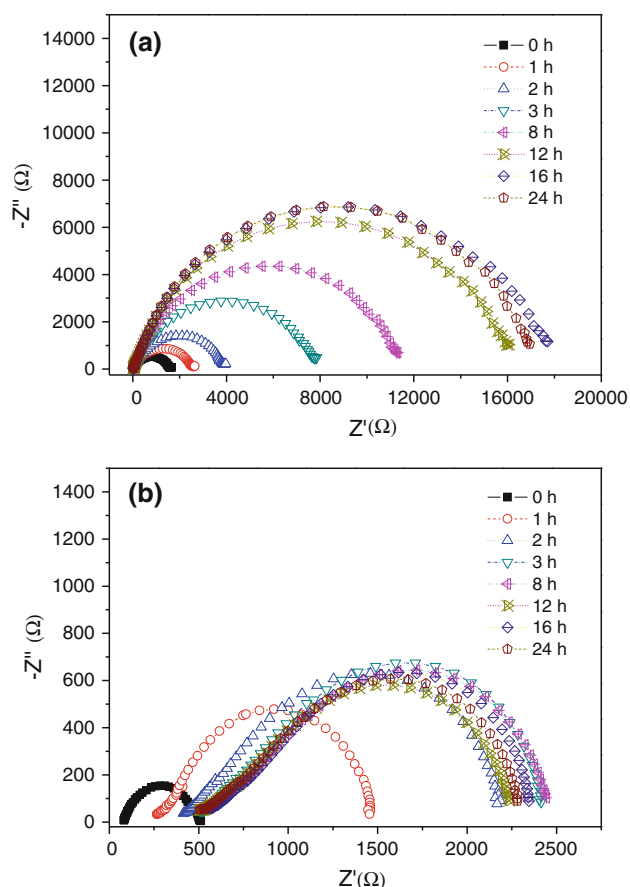


**Fig. 4** Time evolution of the impedance spectra of a symmetric Li/polymer gel electrolyte/Li cell from 0 to 24 h. The polymer gel electrolyte was **a** Sam Blank and **b** Sam B

be produced in the meantime. Further, the passivation film somewhat restrained the reaction between the IL electrolyte and lithium metal, which leads to a dynamic equilibrium state after a period of time at last [20, 21].

### 3.4 Lithium redox

Lithium redox in the polymer gel electrolyte was characterized by cyclic voltammograms (CVs), as shown in Fig. 6. Since the S221TFSI IL has low cathodic stability (1.6 V vs.  $\text{Li}/\text{Li}^+$ ), the lithium plating cannot be produced in the S221TFSI. As a result, a film-forming additive, GBL, has to be added in the electrolyte to avoid its cathodic decomposition and to improve the interfacial compatibility toward the lithium anode. From Fig. 6, highly reversible Li plating/stripping on the nickel electrode can be clearly observed for the two polymer electrolytes. Furthermore, in the first cycle for the two polymer gel electrolytes, the cathodic peak corresponding to the plating of lithium was about  $-0.20$  V versus  $\text{Li}/\text{Li}^+$ , and in the returning scan, the anodic peak corresponding to the stripping of lithium was around  $0.34$  V versus  $\text{Li}/\text{Li}^+$ . The reversible Li plating/stripping on the

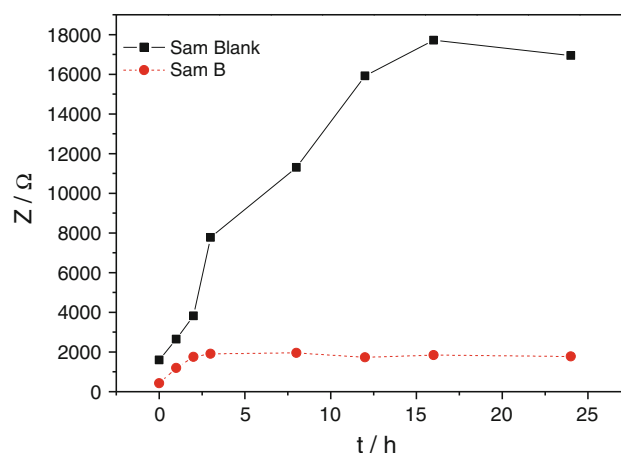


**Fig. 5** Time dependence of interfacial resistance of a symmetric Li/polymer gel electrolyte/Li cell from 0 to 24 h. The polymer gel electrolyte was Sam Blank and Sam B

nickel electrode indicates GBL could generate a certain passivating film (SEI) on the Ni electrode corresponding to the broad cathodic peak, ranging from  $0.72$  to  $-0.10$  V versus  $\text{Li}/\text{Li}^+$ , restraining the further decomposition of the polymer electrolytes in reduction process [18], which was also in agreement with the testing result of interfacial resistance.

### 3.5 Charge–discharge performance of batteries

The Charge–discharge (C–D) performance of Li/polymer electrolytes/ $\text{LiFePO}_4$  batteries had been determined at  $25^\circ\text{C}$ , and their cycling stability is shown in Fig. 7. After an initial increase that may be a result of which the liquid component penetrated gradually into the electrode material [22], the cell delivered a stable capacity. When the liquid electrolyte component in polymer electrolytes was 75 wt%, the discharge capacity of the assembled battery was higher compared with the other batteries. This result is well in agreement with the data of the ion conductivity. Because the polymer gel electrolyte containing 75 wt% liquid electrolyte component has higher ion conductivity than the other samples, the transport efficiency of lithium ions in the polymer electrolyte is higher, resulting in a higher discharge capacity of the battery. After about 60 cycles for the battery with the 0.25 PVdF-HFP/0.75 SE polymer electrolyte, the discharge capacity was stable and reached  $150\text{ mAh g}^{-1}$ . Moreover, after 100 cycles, the discharge capacity of the battery was still higher and it retained  $148\text{ mAh g}^{-1}$ .

In addition, the performance of  $\text{Li}/(0.25\text{ PVdF-HFP}/0.75\text{ SE})/\text{LiFePO}_4$  cell at different current rates was also determined, as shown in Fig. 8. It could be observed that the discharge capacity decreased with an increase in the current rates. For the IL-based polymer electrolytes, the fall



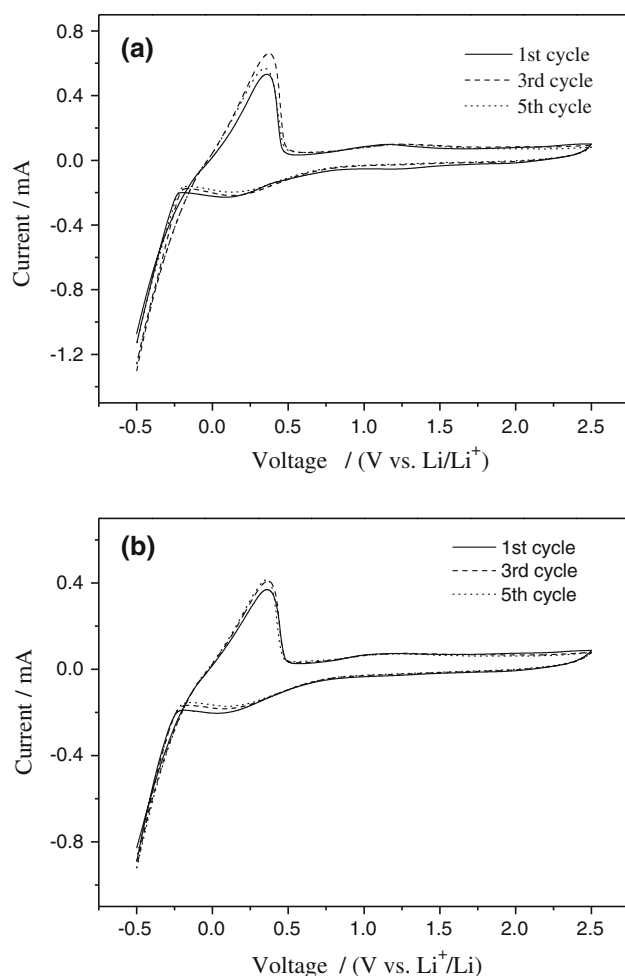


**Fig. 6** Cyclic voltammograms for the polymer electrolytes at 25 °C: **a** 0.25 PVdF-HFP/0.75 SE samples, **b** 0.2 PVdF-HFP/0.8 SE samples. Working electrode: Ni; counter electrode and reference electrode: lithium; scan rate: 10 mV s<sup>-1</sup>

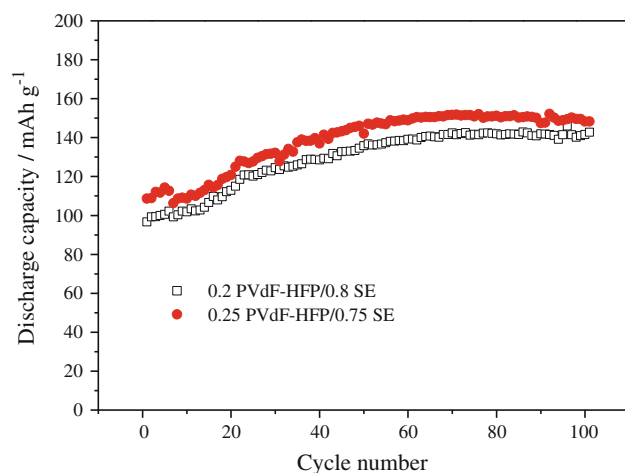


**Fig. 7** Discharge capacity against cycle numbers for Li/polymer gel electrolytes/LiFePO<sub>4</sub> cells at 25 °C. Charge–discharge current rate is 0.1 °C

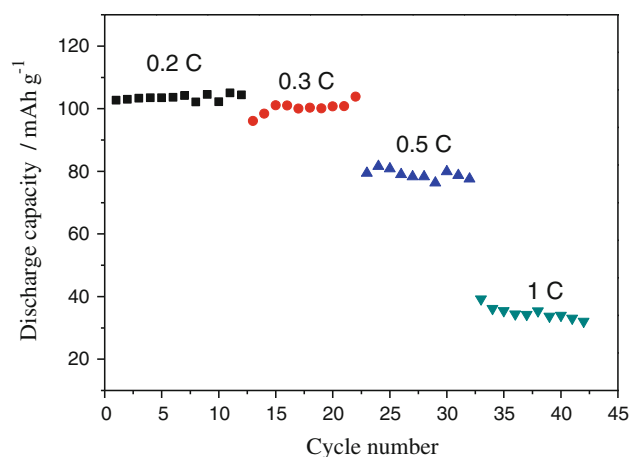


**Fig. 8** Discharge capacities against cycle numbers for Li/(0.25 PVdF-HFP/0.75 SE)/LiFePO<sub>4</sub> cells at different discharge rates at 25 °C. Charge current rate is fixed at 0.1 °C

of discharge capacity at elevated current rates is associated with their low lithium ion transference numbers [18, 23].

A relatively high  $T_{Li+}$  could eliminate the concentration gradients within the battery and could ensure the battery working at high current density [24]. Here,  $T_{Li+}$  value in the quaternary polymer gel electrolyte is 0.06 which is relatively low. However, the discharge capacity of the battery with the polymer electrolyte still reached about 100 mAh g<sup>-1</sup> at 0.3 °C current rates.

#### 4 Conclusion

In this article, polymer gel electrolytes based on the PVdF-HFP as host and incorporating a sulfur-based IL, LiTFSI salt, and a GBL additive have been prepared. The polymer electrolytes had good thermal stability, and they did not decompose until 290 °C. Particularly, the polymer electrolytes exhibited good lithium plating/stripping reversibility. When the liquid electrolyte component reached 75 wt%, the ionic conductivity of the polymer electrolyte was higher and it was  $6.32 \times 10^{-4}$  S cm<sup>-1</sup>. The battery with the polymer electrolyte at 100th cycle could deliver the capacity of 148 mAh g<sup>-1</sup> at 0.1 °C current rates and 25 °C.

**Acknowledgments** The authors are grateful for financial support for this study from the National Basic Research Program of China (973 Program, Grant 2009CB219906), Specialized Research Fund for the Doctoral Program of Higher Education of China (20110201130002), National Natural Science Foundation of China (21276203), and the Postdoctoral Foundation of China (Grants No. 2012M511991).

#### References

- Armand M, Endres F, MacFarlane DR, Ohno H, Scrosati B (2009) Nat Mater 8:621

2. Davis JH (2004) *Chem Lett* 33:1072
3. Hagiwara R, Lee JS (2007) *Electrochemistry* 75:23
4. Kim GT, Appetecchi GB, Alessandrini F, Passerini S (2007) *J Power Sources* 171:861
5. Shin JH, Henderson WA, Scaccia S, Prosini PP, Passerini S (2006) *J Power Sources* 156:560
6. Raghavan P, Zhao X, Manuel J, Chauhan GS, Ahn J-H, Ryu H-S, Ahn H-J, Kim K-W, Nah C (2010) *Electrochim Acta* 55:1347
7. Fung YS, Zhou RQ (1999) *J Power Sources* 81–82:891
8. Yuan J, Antonietti M (2011) *Polymer* 52:1469
9. Koch VR, Nanjundiah C, Battista Appetecchi G, Scrosati B (1995) *J Electrochem Soc* 142:L116
10. Matsumoto H, Yanagida M, Tanimoto K, Nomura M, Kitagawa Y, Miyazaki Y (2000) *Chem Lett* 8:922
11. Ferrari S, Quartarone E, Mustarelli P, Magistris A, Fagnoni M, Protti S, Gerbaldi C, Spinella A (2010) *J Power Sources* 195:559
12. Fisher AS, Khalid MB, Widstrom M, Kofinas P (2011) *J Power Sources* 196:9767
13. Fang S, Yang L, Wei C, Peng C, Tachibana K, Kamijima K (2007) *Electrochem Commun* 9:2696
14. Li M, Yang L, Fang S, Dong S, Jin Y, Hirano S-i, Tachibana K (2011) *J Power Sources* 196:6502
15. Evans J, Vincent CA, Bruce PG (1987) *Polymer* 28:2324
16. Bruce PG, Evans J, Vincent CA (1988) *Solid State Ionics* 28–30 Part2:918
17. Rajendran S, Mahendran O, Mahalingam T (2002) *Eur Polym J* 38:49
18. Ye H, Huang J, Xu JJ, Khalfan A, Greenbaum SG (2007) *J Electrochem Soc* 154:A1048
19. Martinelli A, Matic A, Jacobsson P, Borjesson L, Farnicola A, Panero S, Scrosati B, Ohno H (2007) *J Phys Chem B* 111:12462
20. Raghavan P, Zhao X, Shin C, Baek DH, Choi JW, Manuel J, Heo MY, Ahn JH, Nah C (2010) *J Power Sources* 195:6088
21. Farnicola A, Croce F, Scrosati B, Watanabe T, Ohno H (2007) *J Power Sources* 174:342
22. Shin JH, Henderson WA, Passerini S (2005) *J Electrochem Soc* 152:A978
23. Li M, Yang L, Fang S, Dong S, Hirano S-i, Tachibana K (2012) *Polym Int* 61:259
24. Tarascon JM, Armand M (2001) *Nature* 414:359